9th IAA Planetary Defense Conference – PDC 2025
5–9 May 2025, Stellenbosch, Cape Town, South Africa

IAA-PDC25-07-257

Refining Asteroid Mass Uncertainty via Volume, and Bulk Density Constraints for Optimal Flyby Mission Design

Melissa Buys[a,1,*], Charlie P. Hanner[a,2,*], Brent W. Barbee[b,3]

[a] *University of Maryland, College Park, MD, 20742, USA*
[b] *NASA Goddard Space Flight Center, Greenbelt, MD, 20771, USA*

Abstract

The near-Earth object (NEO) discovery rate has increased in recent years, and the discovery rate is expected to further increase dramatically when new telescope systems such as LSST and NEO Surveyor come online during the next several years. Significant increases in NEO discovery rate makes it more and more likely that an asteroid on an Earth-impacting orbit will be discovered during the next decade. Accurately estimating the mass of Earth impacting asteroids is essential for predicting potential Earth impact effects and designing spacecraft missions to prevent Earth impacts. However, asteroid mass estimates are often clouded with significant uncertainties if the asteroid is only observed by ground-based telescopes. The quickest way to reduce these uncertainties is to send a fast flyby spacecraft mission to reconnoiter the asteroid. Directly measuring asteroid mass with a fast flyby mission is very difficult, but capturing camera images of the asteroid is relatively straightforward. Spacecraft camera images of the asteroid can be used to build a shape model of the asteroid using techniques such as stereophotoclinometry, and that shape model yields an estimate of the asteroid's volume and associated uncertainty. However, without additional measurements or a priori constraints, significant uncertainties remain in the asteroid's base material density and bulk porosity (or, taken together, bulk density).

Asteroid mass can be described as the product function (f) of volume, base material density, and bulk porosity, and an expression can be derived relating percent uncertainty in f to the uncertainty in f's dependent variables. Asteroid volume uncertainty can be significantly reduced by an appropriately designed flyby mission. This begs the question "Given a particular volume uncertainty from processing spacecraft camera images of an asteroid, what are the required a priori uncertainties in bulk porosity and base material density to keep the resulting mass uncertainty below a particular level?". In this study, we explore the interconnected nature of these uncertainties and estimate the lowest asteroid mass uncertainties achievable when only volume measurements are available, based on current abilities to constrain asteroid density and porosity. We also discuss how low the uncertainties on asteroid density and porosity would need to be in order to achieve given levels of asteroid mass uncertainty utilizing only camera imagery collected by fast flyby reconnaissance missions.

The equations and relationships that will be presented can be used to inform asteroid flyby reconnaissance mission design and instrument selection, as they give an indication of the instrument precision and resolution required to achieve a desired goal in asteroid mass uncertainty. Mission implications from a space-systems perspective are explored, helping to inform mission requirements and performance expectations for a given set of estimated asteroid parameters.

Keywords: asteroid flyby, asteroid reconnaissance, mass estimation, mass uncertainty, asteroid 2024 YR4

*Corresponding author
Email addresses: mbuys@umd.edu (Melissa Buys), casper@umd.edu (Charlie P. Hanner), brent.w.barbee@nasa.gov (Brent W. Barbee)
[1] Ph.D. Candidate, Department of Aerospace Engineering
[2] Ph.D., Department of Aerospace Engineering
[3] Lead Planetary Defense Applications Scientist

1. Introduction

Refining the physical properties of asteroids is crucial for designing asteroid mitigation missions and assessing the consequences of possible impacts as part of disaster management and impact response efforts. Near-Earth objects (NEOs) are asteroids and comets whose orbits bring them close to Earth's orbit around the Sun. NEOs have perihelion distances of 1.3 AU or less and range in size from a few meters to approximately 34 kilometers across [1]. Some NEOs have long synodic periods and orbital geometries that could make it difficult for ground-based observations to significantly reduce uncertainties in their physical parameters in the case of potentially hazardous objects [1]. Therefore, it is important to develop heuristic relationships that estimate how much asteroid parameter uncertainty can be reduced through flyby missions.

Asteroid material properties are critical when designing deflection or disruption strategies [2]. A major challenge in asteroid mitigation stems from the lack of *a priori* knowledge about these properties: uncertainties in asteroid shape, density, strength, and internal structure significantly affect how a body will respond to mitigation efforts [2]. For larger asteroids, the effectiveness of a deflection mission heavily depends on early intervention, which requires not only early detection but also continued tracking of potentially hazardous asteroids [2]. Better-constrained uncertainties in asteroid physical parameters would greatly facilitate the design of mitigation spacecraft by providing more precise criteria for mission requirements.

In particular, estimating an asteroid's volume through camera-based observations during a flyby can significantly reduce the uncertainty in calculating its bulk density, while asteroid mass can be determined with high precision by analyzing spacecraft radio tracking data during the flyby [3–8]. As a spacecraft flies past an asteroid, its trajectory is perturbed by the asteroid's gravitational attraction in proportion to the asteroid's mass. However, the magnitude of this perturbation also depends on the encounter design, including the flyby distance, the relative velocity between the spacecraft and the asteroid, and the flyby geometry [3]. While this method is more accurate for larger asteroids, its precision decreases rapidly for smaller bodies [4].

The masses of asteroids such as Mathilde, Eros, and Lutetia have been determined through spacecraft flyby trajectory perturbations [9–11]. The masses of Itokawa and Bennu were determined with rendezvous spacecraft [12, 13]. Accurate mass measurements have also been achieved by analyzing the long-term gravitational effects asteroids exert on neighboring solar system bodies [3, 8]. For example, the masses of Ceres, Pallas, and Vesta were inferred based on their gravitational influences on Mars' orbit [14], and the masses of 243 Ida and 45 Eugenia were estimated by analyzing the motion of their moons [15, 16]. Determining asteroid masses through gravitational interactions often requires solving a high-dimensional inverse problem involving at least thirteen parameters, including the masses and orbital elements of both the perturbing and test asteroids, based on astrometric observations [8]. Larger asteroid masses can also be determined by fitting models to planetary ephemerides [7]; however, these models are less accurate and must incorporate hundreds of asteroids to achieve adequate precision [4, 7].

Except for flyby missions, all methods for determining asteroid mass typically require either precision spacecraft orbits, specific rendezvous instruments, or observations collected over long periods. In a planetary defense scenario—depending on how far in advance the asteroid is discovered—flyby missions may be the only practical option for narrowing uncertainty in physical parameters.

Volume uncertainties obtained from flyby missions typically range from 10% to 30%, making it a key driver in the precision of bulk density estimates and asteroid classification [3, 4]. Mass estimates determined through spacecraft tracking generally have uncertainties of 10% to 15% [4]. The density and internal structure of asteroids are among the least well-constrained parameters[4, 17]. Both mass and volume must be accurately determined to derive an asteroid's density [4, 5, 8]. However, both properties are difficult to measure directly. Indirect estimates of density based on photometric observations of mutual eclipses in small binary near-Earth asteroids do not require prior knowledge of mass or size. However, these estimates are generally much less accurate than those obtained through direct measurement methods [4]. Alternatively, if an asteroid's volume is known, its mass can be roughly estimated by multiplying the volume by the average bulk density associated with its taxonomic class. These class averages are based on measured densities of other asteroids within the same spectral group. However, this approach ignores important factors such as porosity, and the true bulk density of an individual asteroid may differ significantly from the class average. Consequently, such mass estimates are considered rough and not highly reliable [8].Table 1 summarizes previous missions where spacecraft flybys have improved knowledge of asteroid mass and volume.

Table 1: Summary of asteroid and comet missions with estimated mass and volume from fly-by missions.

Mission	Body	Encounter	m (kg)	V (m^3)
NEAR [18]	253 Mathilde	1997	$1.033 \pm 0.044 \times 10^{17}$	$78^{+12}_{-11} \times 10^{12}$
NEAR [19, 20]	433 Eros	1999	$6.687 \pm 0.003 \times 10^{15}$	$2900 \pm 600 \times 10^{9}$
Rosetta [21]	2867 Steins *	2008	$1.368 \times 10^{14} \pm 1.98 \times 10^{13}$	$76 \times 10^{9} \pm 11 \times 10^{9}$
EPOXI [22, 23]	103P/Hartley 2	2010	$242.7 \times 10^{9} \pm 163.5 \times 10^{9}$	$8.2 \times 10^{8} \pm 8 \times 10^{7}$
New Horizons [24]	486958 Arrokoth	2019	7.485×10^{14}	3.185×10^{12}

* These values were obtained using a bulk density assumption of 1800 kg/m^3

The following sections introduce a model designed to estimate the potential reduction in asteroid parameter uncertainties achievable through a spacecraft flyby. We also review the effectiveness of various instrument combinations and measurement strategies in constraining asteroid properties. Finally, the model is applied to asteroid 2024 YR4, demonstrating its utility in planning future flyby missions aimed at improving the characterization of potentially hazardous asteroids.

2. A Quantitative Approach to Mass Uncertainty

The mass of an asteroid (m) can be expressed as a function of its volume (v), and bulk density (ρ), so that

$$m = f(v, \rho). \tag{1}$$

To quantify the mass uncertainty, we take the total differential of the mass with respect to its variables

$$\delta m = \rho \delta v + v \delta \rho. \tag{2}$$

To characterize uncertainty in terms of standard deviations, we assume that δv, and $\delta \rho$ represent the respective standard uncertainties. The standard deviation of mass, σ_m can be calculated as

$$\begin{aligned} \sigma_m^2 &= \rho^2 \sigma_v^2 + v^2 \sigma_\rho^2. \\ \sigma_m &= \sqrt{\rho^2 \sigma_v^2 + v^2 \sigma_\rho^2}. \end{aligned} \tag{3}$$

Next, we define relative uncertainties to determine relationships for the percentage error in mass, volume, and bulk density

$$p_v = \frac{\sigma_v}{v} \Longrightarrow \sigma_v = p_v v \tag{4}$$

$$p_\rho = \frac{\sigma_\rho}{\rho} \Longrightarrow \sigma_\rho = p_\rho \rho \tag{5}$$

$$p_m = \frac{\sigma_m}{m} \Longrightarrow \sigma_m = p_m m \tag{6}$$

where p_v, p_ρ, and p_m are the percentage error in volume, density, and mass respectively. Substituting these relationships into Equation 3 gives

$$p_m = \sqrt{(p_v^2 + p_\rho^2)}. \tag{7}$$

This relationship is useful for evaluating how individual parameter uncertainties contribute to overall mass uncertainty, which is critical for asteroid characterization and mission planning. While volume uncertainty can be significantly reduced through a well-executed flyby, a key question is determining the required a priori uncertainty in bulk density necessary to achieve a target mass uncertainty. To investigate these uncertainties we can rearrange Equation 7:

$$p_\rho = \sqrt{(p_m^2 - p_v^2)}. \tag{8}$$

Table 2: Calculated density uncertainty given uncertainties in mass and volume.

Mass (p_m)	Volume (p_v)	Density (p_ρ)
0.1	0.05	0.087
	0.1	0
0.25	0.05	0.24
	0.1	0.23
	0.2	0.15
	0.25	0
0.5	0.05	0.5
	0.1	0.49
	0.2	0.46
	0.3	0.4
	0.5	0

Table 2 presents the calculated values for density uncertainty based on given uncertainties in mass and volume. Figure 1 illustrates how density uncertainty varies with different combinations of mass and volume uncertainty. For each mass uncertainty level, density uncertainty increases as volume uncertainty increases. This relationship can be used to determine the required instrument precision needed to achieve a target volume uncertainty during a flyby mission, in order to reach a desired mass uncertainty given a known or estimated uncertainty in bulk density. Furthermore, as shown in Equation 8, the condition $p_v < p_m$ must be satisfied.

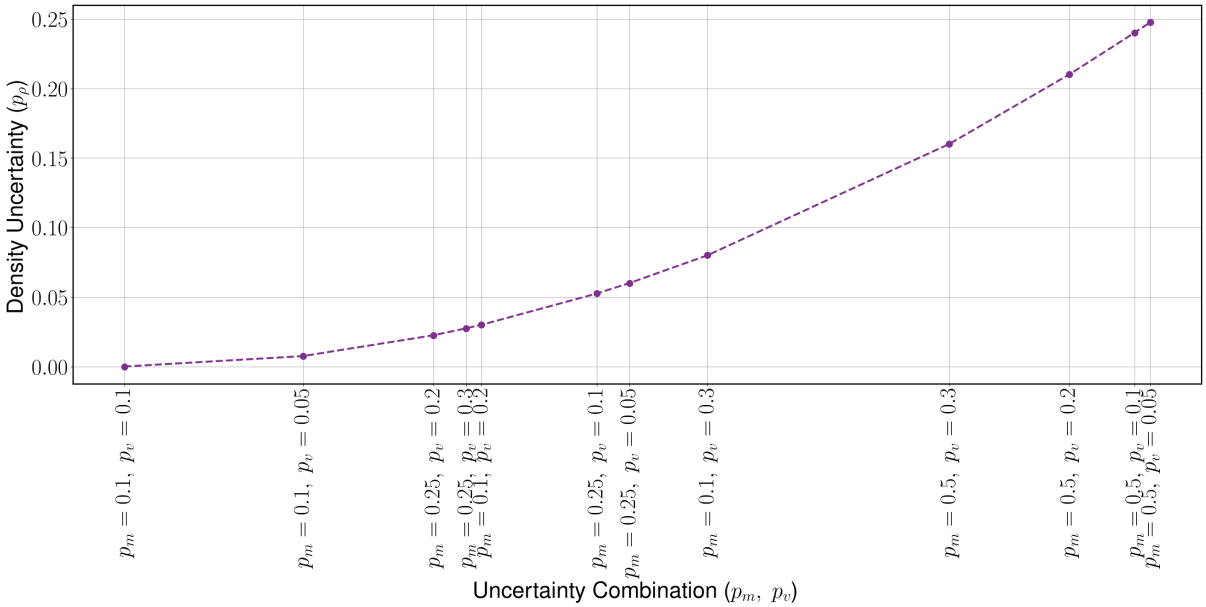

Figure 1: Relationship between mass, volume, and bulk density uncertainty.

3. Implications for Flyby Mission Design

Spacecraft instrumentation categories can be broadly defined for a high-level estimate of their situational benefit in their ability to influence a more focused mass uncertainty estimate.

In estimating a body's volume, most approaches focus in estimating an asteroid's *size* or diameter. Volume sharing relation with diameter by a cubic factor means a factor of 3 relates the uncertainty in diameter to the resultant uncertainty in mass for a given bulk density condition. Given a spherical assumption for an asteroid at a singular density value:

$$V = \frac{\pi}{6} D^3, \quad \ln V = \ln\left(\frac{\pi}{6}\right) + 3 \ln D \tag{9}$$

$$\frac{\partial \ln V}{\partial \ln D} = 3, \quad \frac{\partial V}{V} = 3 \frac{\partial D}{D} \tag{10}$$

While the specific details regarding the spacecraft capabilities, asteroid shape/size, and flyby trajectory are going to affect the specific final result, historical results can be used to generate approximate expectations. The use of visual-spectrum cameras can significantly reduce volume uncertainty when compared to ground-based observation starting point. Stereophotoclinometry (SPC) is a common approach to generating topographical and shape information from 2D images from a spacecraft of a body [25]. Given a set of requirements an uncertainty range can be estimated as shown by Chabot et al. (2024) a flyby of a 50 meter object, illuminating ≥ 10 pixels yields a pixel scale ≤ 5 meters, with a 1 pixel uncertainty per-side resulting in a $\pm$ 10 meter 1-σ uncertainty [26]. This example would result in a 20% 1-σ uncertainty, aligning with the expected upper range from a series of previous flybys. The NEAR spacecraft's flyby of 253 Mathilde, while regarding a significantly larger scale body, was able to achieve a volumetric uncertainty of $\pm 14\%$ [27]. Through only the approach imaging of DART a 25% volume uncertainty was achieved on the ~ 150 m body, signifying a size uncertainty of just $\sim$ 8%. DART's terminal approach imaging is able to reduce volume uncertainty to just $\sim 8\%$ in volume [26]. While this shows flyby imaging can aid to reduce volumetric uncertainty down to below $\leq 10\%$, a more realistic expectation is within the range of $\sim 15 - 20\%$ for approximately spherical asteroids and these values can significantly climb dependent on elongation [28].

The inclusion of an infrared (IR) spectrometer can also have significant effects on the mass uncertainty of an asteroid. The NEOWISE mission has been able to estimate diameters of asteroids to between -13.7% to +18.6% [29]. However the significant benefit in the use of the IR spectrum is in avoiding reliance on absolute magnitude (H) which often has $\geq 30\%$ uncertainties. Spectral classification via IR largely reduces the density uncertainty to the asteroid's porosity in identifying the taxonomoic class [30]. Table 3 shows the ranges for bulk density across the 4 most commonly found taxonomic classes of asteroids as well as the uncertainty percentages largely resulting from porosity variations.

Table 3: Bulk density (mean $\pm 1\sigma$) by asteroid taxonomic class with percentage uncertainty. For values from B. Carry [6], values are reported from the N_{50} estimates class. S-type (silicaceous) asteroids are denser on average than C-type (carbonaceous) asteroids[6]. X-class asteroids span a wide density range[6]; here the mean is representative of the low-albedo P-type subset. M-type asteroids (a subset of X with high radar albedo) have the highest densities, consistent with metal-rich compositions[6].

Taxonomic Class	Bulk Density (Mean $\pm 1\sigma$)	Uncertainty (%)	Examples
S-type	2.70 ± 0.69 g/cm^3 [6]	$\pm$ 25.6%	433 Eros, 25143 Itokawa
C-type	1.41 ± 0.69 g/cm^3 [6]	$\pm$ 48.9%	253 Mathilde, 101955 Bennu
X-type	1.99 ± 0.99 g/cm^3 [6]	$\pm$ 49.7%	87 Sylvia
M-type	3.85 ± 1.27 g/cm^3 [6]	$\pm$ 33.0%	16 Psyche, 216 Kleopatra

IR radiometry may also provide significant insight to the regime of bulk porosity an asteroid may have by comparing the thermal inertia between the sunlit and night hemispheres. If the flyby trajectory permits, quantification of the thermal inertia of the asteroid's surface using an thermal infrared imager can reduce uncertainty by using porosity-inclusive thermal-conductivity models. For example, when classifying Bennu's porosity, the OSIRIS-REx team correlated their high-reflectance boulder thermal inertia value of $\sim$400 to 700 $Jm^{-2}K^{-1}s^{-1/2}$ to an approximate porosity value between 24-38% near the surface layers [31]. While a flyby may not be able to provide as comprehensive of an analysis of porosity as the OSIRIS-REx spacecraft was able to with its rendezvous ($\sim \pm 7\%$), it likely still has significant benefit in eliminating infeasible regions of porosity within the taxonomic classes. The data from JAXA's (Japan Aerospace Exploration Agency) MARA instrument on the surface of Ryugu from observing a full-cycle thermal is able to reduce porosity uncertainty to $\leq \pm 5\%$ given external data regarding particle size, noting the greatest influence in variability reduction comes from night-side observations [32].

Another investigation method, while still untested, is the use of low-frequency radar sounding to provide subsurface estimates of an asteroid's porosity. The Juventas Cubesat is slated to carry the

smallest radar system to be flown in space to perform rendezvous characterization of Dimorphos [33]. The results from Juventas' subsurface scanning efforts are likely to provide strong indications regarding the viability of using a low-power radar like this for flyby missions. If deemed possible, this approach may provide an avenue to reduce porosity uncertainty without requiring observations of both the sun-lit and night portions of an asteroid, alleviating some trajectory design requirements. For the sake of the distribution analysis below it is assumed that the inclusion of one or more of these instruments can reduce the porosity uncertainty to between $\sim 10 - 20\%$. This additionally assumes the majority of the bulk density uncertainty is due to the variance in the asteroid's porosity and that the body is largely homogeneous. Further reduction below 10% may be possible depending on the observations possible from the flyby trajectory, although this has only been demonstrated to this level during rendezvous previously.

Table 4: Expected 1-σ uncertainty reductions in volume and bulk density for different instrument configurations. Values are based on historic flyby missions and provide a high-level estimate of what can be expected. The true reductions will be highly dependent on the final mission design, asteroid size, and instrumentation selected. The reduced volumetric uncertainty from combining instrument approaches is difficult to holistically capture from literature and is highly mission design dependent.

Instrument Configuration	Volumetric Uncertainty (%)	Bulk Density Uncertainty (%)
Camera/IR spectrometer	15–20	25–50 (class-dependent)
IR radiometry/Radar	–	10–20
Combined Instrumentation	~≤15 - 20	10–20

4. Model Evaluation using Asteroid 2024 YR4

2024 YR4 was discovered on December 27, 2024, by the ATLAS telescope in Rio Hurtado, Chile [34, 35]. The asteroid orbits the Sun with a semimajor axis of 2.52 au, an eccentricity of 0.66, and an inclination of 3.41°, and it has a minimum orbit intersection distance with Earth of approximately 0.003 au [34]. From JWST observations, it has been estimated that 2024 YR4 is an S-type asteroid [36]. After discovery, the JPL/CNEOS Sentry impact monitoring system identified a potential impact event of 2024 YR4 on December, 22, 2032 with an estimated impact probability of 1.2% [35, 37]. By February 2025, the impact probability risk reached a peak at 2.8% after which it dropped down to 0.001% following observations made by the European Southern Observatory's Very Large Telescope [38]. While the risk to Earth has been effectively ruled out, there remains a 1.7% chance of 2024 YR4 impacting the Moon on December, 22, 2032 [39]. Table 5 below lists the absolute magnitude, albedo, and density properties of 2024 YR4.

These properties have been used with the algorithm from section 2 to investigate how the model can be useful when designing mitigation missions for potentially hazardous objects.

Table 5: Physical properties of 2024 YR4

	Value	Note
H-Magnitude	24.05 ± 0.15 [36, 40]	After rotation lightcurve correction
Albedo	0.197 ± 0.051 [41]	Mean albedo for S/A/L types of size 0.6 - 200 km
Density [g/cm^3]	2.70 ± 0.69 [6]	Based on 28 estimates with a 50% accuracy

4.1. Baseline Distribution Calculation

A Monte Carlo simulation can be performed to estimate the asteroid 2024 YR4's diameter distribution by sampling its albedo and absolute magnitude distributions. These samples can then be used with the empirical relation for diameter estimation from Harris (1997) [42]:

$$d = 10^{3.1235 - 0.5 \log_{10}(a) - 0.2\,H} \times 10^3 \quad \text{(m)} \tag{11}$$

Both the albedo and absolute magnitude are treated as having Gaussian distributions, and as a result are sampled as $a \sim \mathcal{N}(0.197, 0.051^2)$ with rejection for $a \leq 0$, and $H \sim \mathcal{N}(24.05, 0.15^2)$. Each distribution is taken with $N = 100{,}000$ samples, and by the Central Limit Theorem, the sampling error on the mean diameter can be found:

$$\mathrm{SE}_{\bar{d}} = \frac{\sigma_d}{\sqrt{N}} \approx 0.0268 \text{ m} \tag{12}$$

Figure 2 presents side-by-side panels of the albedo, absolute magnitude, and resulting diameter distributions. For the diameter, the kernel density estimate (KDE) is highlighted in red, with the skewness and excess kurtosis of the diameter noted as they are significantly different than the normal distribution of its constituent variables. Additionally, within the diameter distribution a purple highlighted region appears segmenting out a portion of the distribution. From the March 2025 James Webb Space Telescope (JWST) observations a new, IR-informed, diameter set was published focusing in the 60 ± 7 meter range [43]; this range is colorized in Figure 2 and shows this portion does not lie within the region of the largest probability density.

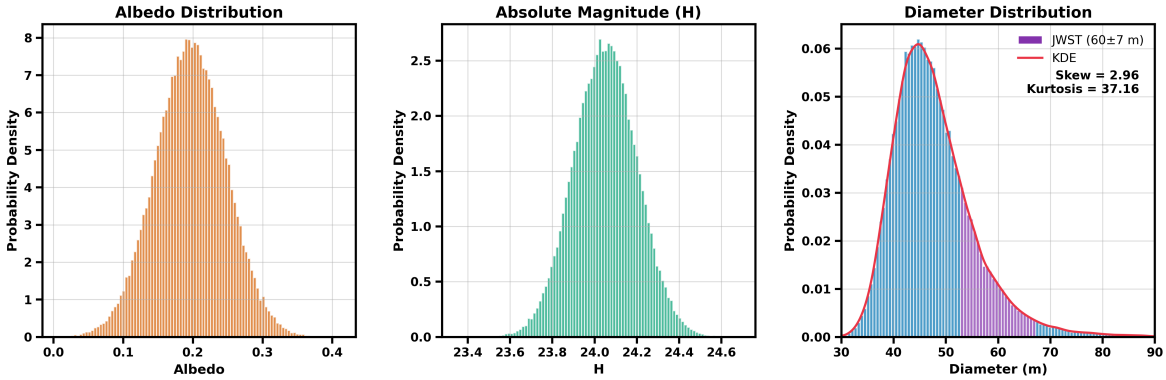

Figure 2: Randomly sampled distributions of 2024 YR4's albedo, absolute magnitude, and resulting diameter. Through the empirical relation $d(\alpha, H)$ the diameter distribution acquires a significant positive skew of ~ 2.96. The diameter distribution also features colorization to highlight the updated uncertainty range following JWST's March observations. This colorization is only included to highlight the subset of the heuristic-based distribution, and is not representative of the full IR-based distribution these observations produced.

Converting the diameter distribution to a volumetric distribution using a spherical assumption provides a baseline starting 1σ uncertainty of *149.04%*. This then provides a baseline setup to complete the analysis regarding the impact of flyby instrumentation in lowering the mass uncertainty of 2024 YR4. A set of four scenarios are selected as seen in Table 6, also capturing the pre-flyby scenario as 2024 YR4 has been identified as of the S-type taxonomic class. The midrange value of the uncertainty ranges as shown in Table 4 are selected for each configuration except for the volumetric uncertainty in the combined instrumentation case. While it is likely that combined instruments provide further refinement of this variance, this analysis utilizes a conservative assumption in no further reduction.

Table 6: Example $\pm 1\sigma$ uncertainties for each flyby scenario regarding 2024 YR4. Colorized via the plotted distribution colors in Figure 3.

Instrument Configuration	Volumetric Uncertainty (%)	Bulk Density Uncertainty (%)
No Flyby Baseline	149.04	25.6
Camera/IR spectrometer	17.5	25.6
IR radiometry/Radar	149.04	15.0
Combined Instrumentation	17.5	15.0

The volumetric uncertainty was assumed to be of the same shape as the pre-flyby, positively-skewed distribution just with the updated variance value. The bulk density is also assumed to be in this scenario centered around the same mean and of a normal-distribution form. The resulting mass probability distribution function for each flyby scenario is shown in Figure 3.

The relative influence of the volume and bulk density uncertainty within each scenario can be evaluated using equation 7. The fractional contributions, or Sobol Indices, can be calculated for each scenario with the following equation set:

$$S_v = \frac{p_v^2}{p_v^2 + p_\rho^2} \tag{13a}$$

$$S_\rho = \frac{p_\rho^2}{p_v^2 + p_\rho^2} \tag{13b}$$

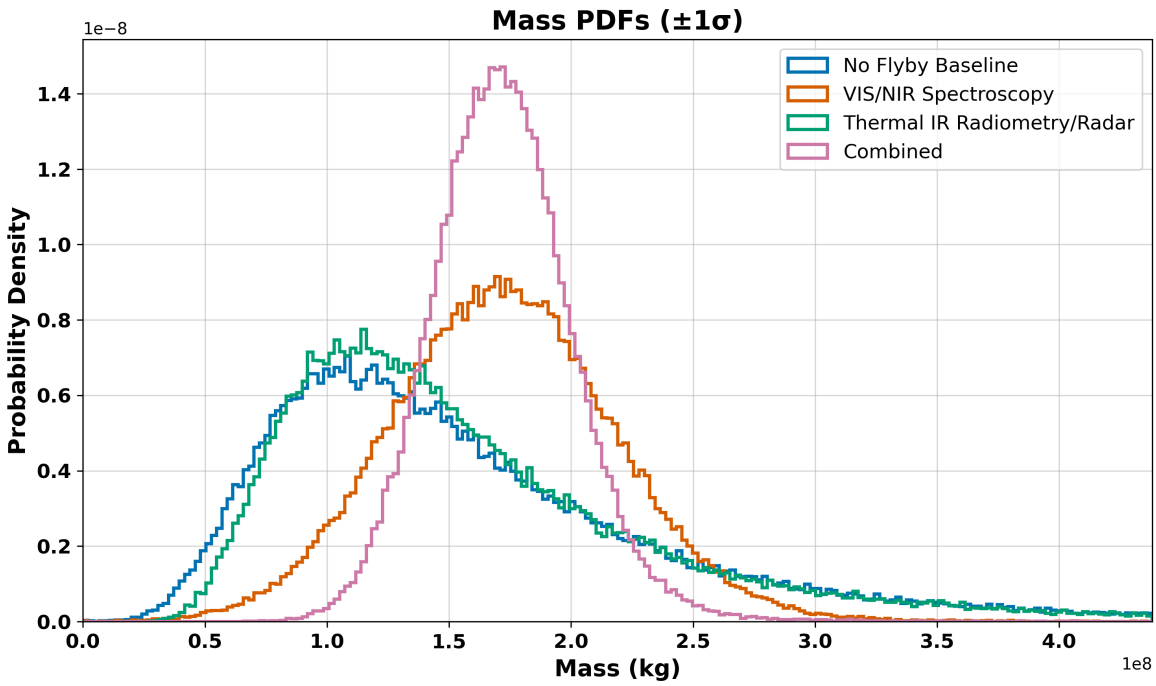

Figure 3: Estimated resulting mass probability distribution for each scenario outlined in Table 6.

1. No-Flyby Baseline

$$p_{v,\text{prior}} \approx 1.49, \quad p_{\rho,\text{prior}} \approx 0.256 \quad \Longrightarrow \quad p_{m,\text{prior}} = \sqrt{1.49^2 + 0.256^2} \approx 1.51\ (151\%),$$

$$S_{v,\text{prior}} = \frac{1.49^2}{1.49^2 + 0.256^2} \approx 0.97\ (97\%), \quad S_{\rho,\text{prior}} = \frac{0.256^2}{1.49^2 + 0.256^2} \approx 0.03\ (3\%).$$

These values indicate the volumetric uncertainty contributes to ~ 97% of the mass uncertainty, whereas the bulk density is responsible for ~ 3%.

2. VIS +NIR Spectroscopy

$$p_v = 0.175, \quad p_\rho = 0.256 \quad \Rightarrow \quad p_m = \sqrt{0.175^2 + 0.256^2} \approx 0.310\ (31.0\%),$$

$$S_v \approx \frac{0.175^2}{0.175^2 + 0.256^2} \approx 0.32, \quad S_\rho \approx 0.68.$$

Here the density uncertainty contribution is significantly increased to contribute to ~68% of the remaining mass-uncertainty.

3. Thermal IR Radiometry/Radar

$$p_v = 1.49, \quad p_\rho = 0.15 \quad \Rightarrow \quad p_m = \sqrt{1.49^2 + 0.15^2} \approx 1.50\ (150\%),$$

$$S_v \approx \frac{1.49^2}{1.49^2 + 0.15^2} \approx 0.99, \quad S_\rho \approx 0.01.$$

Reducing density alone appears to have a near negligible effect by itself, reducing responsibility from 3% to 1%.

4. All Instruments Combined

$$p_v = 0.175, \quad p_\rho = 0.15 \quad \Longrightarrow \quad p_m = \sqrt{0.175^2 + 0.15^2} \approx 0.230\ (23.0\%).$$

$$S_v = \frac{0.175^2}{0.175^2 + 0.15^2} \approx 0.576\ , \quad S_\rho \approx 0.424.$$

These results show, for 2024 YR4, initial mission design should likely prioritize reducing volume uncertainty (e.g. SPC imaging), followed by targeted improvements in bulk-density/porosity constraints to push p_m to ~20 % and below.

5. Conclusion

Minimizing uncertainties in the physical parameters of potentially hazardous asteroids is critical for effective planetary defense mission design. By deriving a quantitative relationship between volume, bulk density, and mass, we demonstrate that spacecraft imaging alone can significantly reduce mass uncertainty, provided appropriate instrument resolution and flyby geometry are achieved. However, unless supplemented with data from infrared spectroscopy, thermal radiometry, or radar, uncertainties in bulk density will dominate the residual mass uncertainty.

Beyond quantifying the contribution of each component to mass uncertainty within the selected application to 2024 YR4, a roadmap can be developed from these results regarding mission design. First, significant reductions in mass uncertainty only come once volume is constrained significantly below traditional ground-based observation and current telescope-based estimates ($\sigma_v \leq\sim 20\% \rightarrow \sigma_d \leq\sim 6.\overline{6}\%$); any investment in measurements focused in refining porosity estimation within a taxonomic class before this threshold yields almost no discernible benefit, especially to decision makers. Once volumetric uncertainty is reduced to these levels, further gains begin to require targeting the asteroid's density and porosity as to not bottleneck the estimation. In the combined-instrumentation case, the near-even split (41% vs 59%) between volume and density contributions highlights a regime of diminishing returns: pushing mass-uncertainty below say ~15% is likely to demand simultaneous, high-precision advances in both shape estimation/modeling and bulk-density characterization from the very limited time a flyby offers.

Applying this framework to asteroid 2024 YR4 showed that pre-flyby mass uncertainty is overwhelmingly driven by large volume uncertainties derived from albedo, and absolute magnitude estimates. A flyby mission with imaging only can dramatically reduce this uncertainty, shifting the limiting factor to bulk density uncertainty. Incorporating instruments capable of constraining porosity, such as infrared radiometers of radar, further reduces mass uncertainty, particularly when combined with visual and near-infrared spectral data.

References

[1] R. Landis and L. Johnson. "Advances in planetary defense in the United States". In: *Acta Astronautica* 156 (2019), pp. 394–408. ISSN: 00945765. DOI: 10.1016/j.actaastro.2018.06.020.

[2] D. S. P. Dearborn et al. "Options and uncertainties in planetary defense: Impulse-dependent response and the physical properties of asteroids". In: *Acta Astronautica* 166 (2020), pp. 290–305. ISSN: 0094-5765. DOI: 10.1016/j.actaastro.2019.10.026.

[3] R. Schulz et al. "Rosetta fly-by at asteroid (21) Lutetia: An overview". In: *Planetary and Space Science* 66.1 (2012), pp. 2–8. ISSN: 00320633. DOI: 10.1016/j.pss.2011.11.013.

[4] J. Hanuš et al. "Volumes and bulk densities of forty asteroids from ADAM shape modeling". In: *Astronomy & Astrophysics* 601 (2017), A114. ISSN: 0004-6361, 1432-0746. DOI: 10.1051/0004-6361/201629956.

[5] L. Siltala and M. Granvik. "Asteroid mass estimation with the robust adaptive Metropolis algorithm". In: *Astronomy & Astrophysics* 633 (2020), A46. ISSN: 0004-6361, 1432-0746. DOI: 10.1051/0004-6361/201935608.

[6] B. Carry. "Density of asteroids". In: *Planetary and Space Science*. Solar System science before and after Gaia 73.1 (2012), pp. 98–118. ISSN: 0032-0633. DOI: 10.1016/j.pss.2012.03.009.

[7] Z Murray. "The Challenge of Measuring Asteroid Masses with Gaia DR2 Astrometry". In: *The Planetary Science Journal* 4.12 (2023), p. 239. ISSN: 2632-3338. DOI: 10.3847/PSJ/ad0be5.

[8] L. Siltala and M. Granvik. "Asteroid mass estimation using Markov-chain Monte Carlo". In: *Icarus* 297 (2017), pp. 149–159. ISSN: 0019-1035. DOI: 10.1016/j.icarus.2017.06.028.

[9] D. K. Yeomans et al. "Estimating the Mass of Asteroid 253 Mathilde from Tracking Data During the NEAR Flyby". In: *Science* 278.5346 (1997), pp. 2106–2109. DOI: 10.1126/science.278.5346.2106.

[10] D. K. Yeomans et al. "Estimating the Mass of Asteroid 433 Eros During the NEAR Spacecraft Flyby". In: *Science* 285.5427 (1999), pp. 560–561. DOI: 10.1126/science.285.5427.560.

[11] M. Pätzold et al. "Asteroid 21 Lutetia: Low Mass, High Density". In: *Science* 334 (2011), p. 491. ISSN: 0036-8075. DOI: 10.1126/science.1209389.

[12] S. Abe et al. "Mass and Local Topography Measurements of Itokawa by Hayabusa". In: *Science* 312.5778 (2006), pp. 1344–1347. DOI: 10.1126/science.1126272.

[13] S. Goossens et al. “Mass and Shape Determination of (101955) Bennu Using Differenced Data from Multiple OSIRIS-REx Mission Phases”. In: *The Planetary Science Journal* 2.6 (2021), p. 219. ISSN: 2632-3338. DOI: 10.3847/PSJ/ac26c4.

[14] E. M. Standish and R. W. Hellings. “A determination of the masses of Ceres, Pallas, and Vesta from their perturbations upon the orbit of Mars”. In: *Icarus* 80.2 (1989), pp. 326–333. ISSN: 0019-1035. DOI: 10.1016/0019-1035(89)90143-7.

[15] M. J. S. Belton et al. “Bulk density of asteroid 243 Ida from the orbit of its satellite Dactyl”. In: *Nature* 374.6525 (1995), pp. 785–788. ISSN: 1476-4687. DOI: 10.1038/374785a0.

[16] W. J. Merline et al. “Discovery of a moon orbiting the asteroid 45 Eugenia”. In: *Nature* 401.6753 (1999), pp. 565–568. ISSN: 1476-4687. DOI: 10.1038/44089.

[17] A. Matter et al. “Determination of physical properties of the Asteroid (41) Daphne from interferometric observations in the thermal infrared”. In: *Icarus* 215.1 (2011), pp. 47–56. ISSN: 0019-1035. DOI: 10.1016/j.icarus.2011.07.012.

[18] J. Veverka et al. “NEAR Encounter with Asteroid 253 Mathilde: Overview”. In: *Icarus* 140.1 (July 1, 1999), pp. 3–16. ISSN: 0019-1035. DOI: 10.1006/icar.1999.6120.

[19] D. K. Yeomans et al. “Radio Science Results During the NEAR-Shoemaker Spacecraft Rendezvous with Eros”. In: *Science* 289.5487 (Sept. 22, 2000), pp. 2085–2088. DOI: 10.1126/science.289.5487.2085.

[20] J Veverka et al. “Imaging of Asteroid 433 Eros During NEAR’s Flyby Reconnaissance”. In: *Science (New York, N.Y.)* 285 (1999), pp. 562–4. DOI: 10.1126/science.285.5427.562.

[21] L. Jorda et al. “Asteroid (2867) Steins: Shape, Topography and Global Physical Properties from OSIRIS Observations”. In: *Icarus* 221.2 (2012), pp. 1089–1100. ISSN: 0019-1035. DOI: 10.1016/j.icarus.2012.07.035.

[22] M.F. A’Hearn et al. “EPOXI at Comet Hartley 2”. In: *Science* 332.6036 (2011), pp. 1396–1400. DOI: 10.1126/science.1204054. URL: https://www.science.org/doi/full/10.1126/science.1204054.

[23] P.C. Thomas et al. “Shape, density, and geology of the nucleus of Comet 103P/Hartley 2”. In: *Icarus*. Stardust/EPOXI 222.2 (2013), pp. 550–558. ISSN: 0019-1035. DOI: 10.1016/j.icarus.2012.05.034.

[24] J. T. Keane et al. “The Geophysical Environment of (486958) Arrokoth—A Small Kuiper Belt Object Explored by New Horizons”. In: *Journal of Geophysical Research: Planets* 127.6 (2022). ISSN: 2169-9100. DOI: 10.1029/2021JE007068.

[25] E. E. Palmer et al. “Practical Stereophotoclinometry for Modeling Shape and Topography on Planetary Missions”. In: *The Planetary Science Journal* 3.5 (2022), p. 102. ISSN: 2632-3338. DOI: 10.3847/PSJ/ac460f.

[26] N. L. Chabot et al. “A Mission to Demonstrate Rapid-Response Flyby Reconnaissance for Planetary Defense”. In: *IAF Symposium on Planetary Defense and Near-Earth Objects*. 2024, pp. 1–9. DOI: 10.52202/078387-0001. arXiv: 2504.15321 [astro-ph]. URL: http://arxiv.org/abs/2504.15321 (visited on 04/27/2025).

[27] J. Veverka et al. “NEAR Encounter with Asteroid 253 Mathilde: Overview”. In: *Icarus* 140.1 (1999), pp. 3–16. ISSN: 0019-1035. DOI: 10.1006/icar.1999.6120.

[28] M. Pätzold et al. “Pre-Flyby Estimates of the Precision of the Mass Determination of Asteroid (21) Lutetia from Rosetta Radio Tracking”. In: *Astronomy & Astrophysics* 518 (2010), p. L156. ISSN: 0004-6361, 1432-0746. DOI: 10.1051/0004-6361/201014325.

[29] N. Myhrvold. “An Empirical Examination of WISE/NEOWISE Asteroid Analysis and Results”. In: *Icarus* 314 (2018), pp. 64–97. ISSN: 0019-1035. DOI: 10.1016/j.icarus.2018.05.004.

[30] H.J. Melosh et al. *Read ”Finding Hazardous Asteroids Using Infrared and Visible Wavelength Telescopes” at NAP.Edu*. National Academies Press, 2019. DOI: 10.17226/25476.

[31] B. Rozitis et al. “Asteroid (101955) Bennu’s Weak Boulders and Thermally Anomalous Equator”. In: *Science Advances* 6.41 (Oct. 8, 2020), eabc3699. ISSN: 2375-2548. DOI: 10.1126/sciadv.abc3699. pmid: 33033037. URL: https://www.ncbi.nlm.nih.gov/pmc/articles/PMC7544501/ (visited on 04/27/2025).

[32] Kazunori Ogawa et al. “Possibility of Estimating Particle Size and Porosity on Ryugu through MARA Temperature Measurements”. In: *Icarus* 333 (Nov. 15, 2019), pp. 318–322. ISSN: 0019-1035. DOI: 10.1016/j.icarus.2019.06.014. URL: https://www.sciencedirect.com/science/article/pii/S0019103518305852 (visited on 04/28/2025).

[33] European Space Agency. *Radar Journey to Centre of Hera’s Asteroid with Juventas CubeSat*. URL: https://www.esa.int/Space_Safety/Hera/Radar_journey_to_centre_of_Hera_s_asteroid_with_Juventas_CubeSat# (visited on 04/27/2025).

[34] B.T. Bolin et al. “The Discovery and Characterization of Earth-crossing Asteroid 2024 YR4”. In: *The Astrophysical Journal Letters* 984.1 (2025), p. L25. ISSN: 2041-8205. DOI: 10.3847/2041-8213/adc910.

[35] R. Park. *Asteroid 2024 YR4 reaches level 3 on the Torino Scale*. 2025. URL: https://cneos.jpl.nasa.gov/news/news210.html (visited on 04/27/2025).

[36] A. S. Rivkin et al. “JWST Observations of Potentially Hazardous Asteroid 2024 YR4”. In: *Research Notes of the AAS* 9.4 (2025), p. 70. ISSN: 2515-5172. DOI: 10.3847/2515-5172/adc6f0.

[37] European Space Agency. *ESA actively monitoring near-Earth asteroid 2024 YR4*. 2025. URL: https://www.esa.int/Space_Safety/Planetary_Defence/ESA_actively_monitoring_near-Earth_asteroid_2024_YR4?utm_source=chatgpt.com (visited on 04/27/2025).

[38] European Space Agency. *Asteroid 2024 YR4 no longer poses significant impact risk*. 2025. URL: https://www.esa.int/Space_Safety/Planetary_Defence/Asteroid_2024_YR4_no_longer_poses_significant_impact_risk (visited on 04/27/2025).

[39] NASA. *Latest Calculations Conclude Asteroid 2024 YR4 Now Poses No Significant Threat to Earth in 2032 and Beyond – Planetary Defense*. 2025. URL: https://blogs.nasa.gov/planetarydefense/2025/02/24/latest-calculations-conclude-asteroid-2024-yr4-now-poses-no-significant-threat-to-earth-in-2032-and-beyond/ (visited on 04/27/2025).

[40] M. Devogèle et al. *Physical characterization of 2024 YR4*. Near Earth Coordination Center ESA ESRIN Frascati Italy, 2025. URL: https://iawn.net/documents/20250204_20th_Vienna/ESA-S2P-PD-HO-0262.pdf.

[41] P. Pravec et al. "Absolute magnitudes of asteroids and a revision of asteroid albedo estimates from WISE thermal observations". In: *Icarus* 221.1 (2012), pp. 365–387. ISSN: 0019-1035. DOI: 10.1016/j.icarus.2012.07.026.

[42] A. W. Harris. "On the Revision of Radiometric Albedos and Diameters of Asteroids". In: *Icarus* 126.2 (Apr. 1, 1997), pp. 450–454. ISSN: 0019-1035. DOI: 10.1006/icar.1996.5664.

[43] A.S. Rivkin et al. *JWST Observations of Potential Impactor 2024 YR4*. Unpublished technical memo. Mar. 27, 2025. URL: https://iawn.net/obscamp/2024YR4/gallery/YR4_memo_final_27mar25.pdf.